

## HHFW AND EBW RESEARCH ON NSTX

B.P. LeBlanc<sup>1</sup>, R.E. Bell<sup>1</sup>, S. Bernabei<sup>1</sup>, J.B. Caughman<sup>4</sup>, L. Delgado-Aparicio<sup>3</sup>, S.J. Diem<sup>1</sup>,  
P.C. Efthimion<sup>1</sup>, R.W. Harvey<sup>6</sup>, J.C. Hosea<sup>1</sup>, C. K. Phillips<sup>1</sup>, J. Preinhaelter<sup>5</sup>, P.M. Ryan<sup>4</sup>,  
S. Sabbagh<sup>2</sup>, G. Taylor<sup>1</sup>, K. Tritz<sup>3</sup>, J. Urban<sup>5</sup>, J.B. Wilgen<sup>4</sup>, J. R. Wilson<sup>1</sup> and the NSTX  
team

<sup>1</sup>PPPL, Princeton, USA, <sup>2</sup>Columbia U., New York, USA

<sup>3</sup>JHU, Baltimore, USA, <sup>4</sup>ORNL, Oak Ridge, USA

<sup>5</sup>Czech Institute of Plasma Physic, Prague, Czech Republic

<sup>6</sup>CompX, Del Mar, USA

### INTRODUCTION

The RF program on NSTX contains two main elements aimed at coupling power for plasma heating and current drive. The high-harmonic fast wave (HHFW) program has been supporting NSTX's research program since its inception and the electron Bernstein wave (EBW) program was initiated later in order to assist and complement some of the functions rendered by HHFW, with emphasis on localized off-axis current drive. The present EBW research involves modeling current drive and coupling physics and coupling studies via EBW emission measurements. Work has begun on a high power EBW heating system.

### HHFW RESEARCH

Recently the operational toroidal field,  $B_T$ , on NSTX has been increased to 5.5 kG, a  $\approx 20\%$  increase over the previous 4.5 kG limit. The higher  $B_T$  resulted in markedly improved HHFW heating performance. Central  $T_e$  of 4 keV, was obtained with 1.9 MW of RF power with a launch toroidal wavenumber,  $k_{\parallel} = -7 \text{ m}^{-1}$ , which is expected to drive current. Figure 1 shows a  $T_e(R)$  comparison of such a plasma and an ohmic reference discharge. Previously<sup>1</sup>, at  $B_T = 4.5$  kG, this level of heating was only obtained with a purely heating  $k_{\parallel} = 14 \text{ m}^{-1}$ . Furthermore the new experimental data set contributed to better understanding of the antenna-plasma coupling physics. This subject is particularly important, because significant edge losses – 10 to 30% – had been observed earlier<sup>2,3</sup>, an effect that worsens with lower  $k_{\parallel}$  for  $B_T = 4.5$  kG. We use a HHFW modulation technique<sup>4</sup> to evaluate the power,  $\Delta P_{\alpha}$ , absorbed by the magnetically enclosed plasma. The index  $\alpha$  refers to plasma species, namely  $e$  for electrons or  $p$  for whole

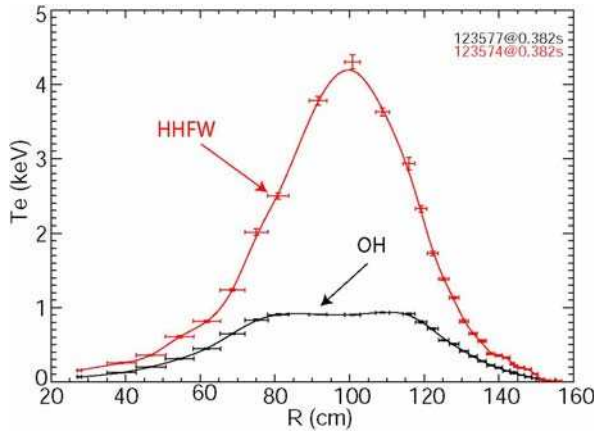


Fig. 1. Overlay of  $T_e(R)$  for plasma with 1.8-MW HHFW at  $k_{//} = -7 \text{ m}^{-1}$  and ohmic reference discharge at  $t=0.382 \text{ s}$ .

0.65 compared to  $\sim 0.44$  at the lower  $B_T$ . But looking at the first power pulse, we observe a  $k_{//}$  heating scaling:  $\Delta W_e(/7 \text{ m}^{-1}) \approx \Delta W_e(14 \text{ m}^{-1})/2$ , similar to the 4.5 kG results. Figure 3 shows a time evolution of the electron density,  $n_e$ , measured by Thomson scattering at a major radius 2 cm in front of the antenna Faraday shield and outside of the last closed flux surface, LCFS, for the discharges shown in Fig. 2. Also indicated in Fig. 3 is the density level for onset of fast wave propagation at  $k_{//}$  of  $-7 \text{ m}^{-1}$  and  $14 \text{ m}^{-1}$ ; this “onset  $n_e$ “ is proportional<sup>5</sup> to  $B \cdot k_{//}^2$ .

One notices that the measured  $n_e$  are significantly lower during the last two pulses than during the first one, when  $n_e$  is clearly above the onset level for  $k_{//} = -7 \text{ m}^{-1}$ . Hence the wave

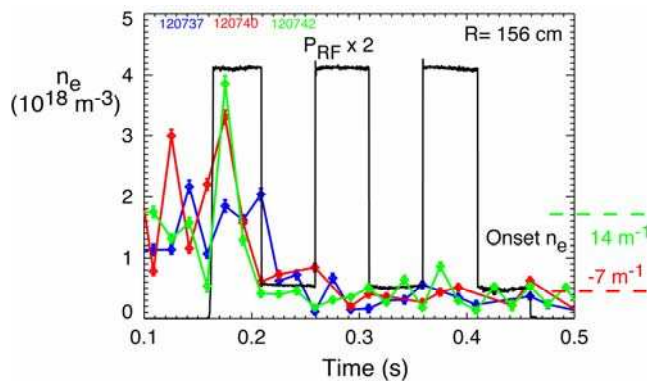


Fig. 3. Edge electron density (2 cm in front of Faraday shield) against time corresponding to curves in Fig 1.

plasma. A heating efficiency parameter is defined  $\eta \equiv \Delta P_\alpha / \Delta P_{RF}$ , where  $\Delta P_{RF}$  is the incremental HHFW power. Figure 2 compares the electron stored energy,  $W_e$ , obtained with  $k_{//} = -7, 7, \text{ and } 14 \text{ m}^{-1}$  at 5.5 kG. Looking at the last two power pulses, we see that  $W_e$  is insensitive to these  $k_{//}$  values at  $B_T = 5.5 \text{ kG}$ . Also  $\eta_e \sim 0.4$  at  $k_{//} = -7 \text{ m}^{-1}$  corresponding to a near doubling over  $\eta_e \sim 0.22$  at 4.5 kG; similarly  $\eta_p \sim$

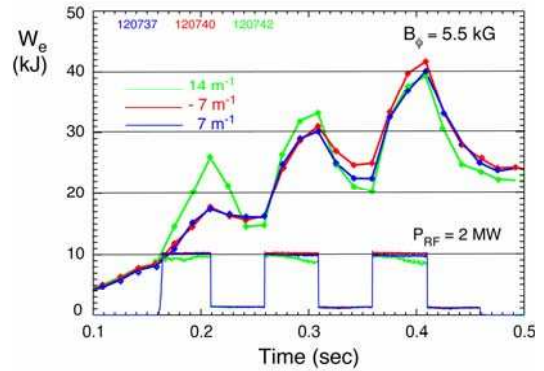


Fig. 2. Electron stored energy versus time and  $k_{//}$  at  $B_T = 5.5 \text{ kG}$ .

propagation started farther away from the LCFS during the first pulse than during the later ones. The previously surmised paradigm of a reduction in parametric decay instability, PDI, losses at the higher  $B_T$  to account for the improved heating efficiency at  $-7 \text{ m}^{-1}$  is not supported by the ERD<sup>6</sup> data in Fig.4 that shows edge ion heating to be a very weak function of  $B_T$ . A more viable

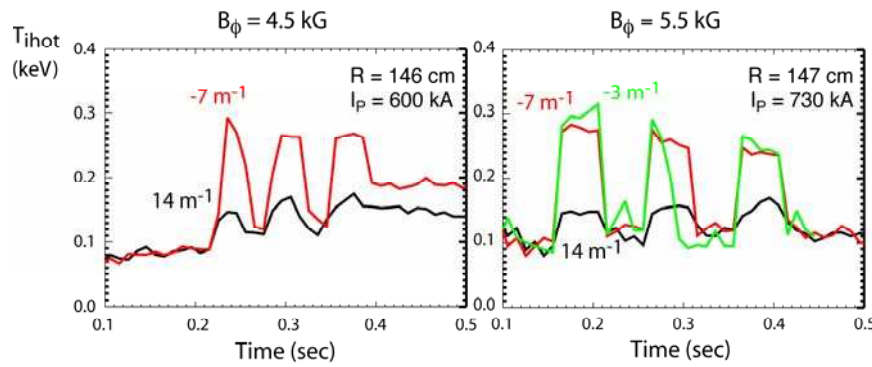


Fig 4. Edge ion heating as a measure of PDI losses. (Helium)

explanation for the edge power loss behavior is the dependency of the fast-wave onset density on  $B$  and  $k_{\parallel}$ , and the loss-prone toroidal propagation of these waves into the outer

scrape-off layer and near the vessel/antenna hardware. Additional work is needed to establish the mechanisms by which power is lost during this surface propagation

### EBW RESEARCH

Central to the issue of EBWCD is how efficiently power can be coupled from externally generated microwave beams to these electrostatic waves. One way to ascertain the coupling efficiency,  $C_E$ , is to investigate the inverse process by which thermal EBW emission is coupled to electromagnetic waves. In the present work the process known as oblique B-X-O coupling is studied<sup>7</sup>. An electron Bernstein wave is transformed into a slow X wave, which itself is mode converted into an O-mode wave. The B-X-O emission diagnostic on NSTX consists of two remotely steered, quad-ridged horn antennas, each coupled to a dual channel radiometer<sup>8</sup>. A detailed mapping of the B-X-O coupling window in NSTX plasmas was accomplished<sup>9</sup> by scanning the antennas in poloidal and toroidal angles while running a sequence of similar L-mode discharges with a plasma current of  $I_p=0.8$  MA, central electron

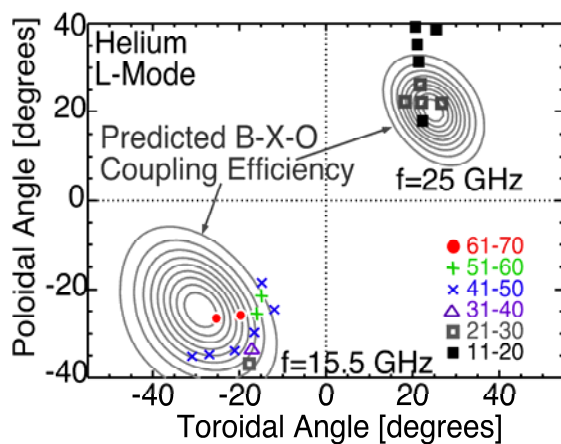


Fig. 5. Conversion efficiency at 15.5 and 25 GHz: grey contours, predicted; colored symbols, measured in L-mode plasmas

temperature  $T_e(0)\sim 1.5$  keV and central electron density  $n_e(0)\sim 3\times 10^{19}$  m<sup>-3</sup>. The antenna was moved to a new toroidal and poloidal pointing angle between discharges. The results of this experiment are shown in Fig. 5 for two frequencies: 15.5 GHz (fundamental) and 25 GHz (second harmonic) along with the predicted contours of mode conversion efficiency. The maximum mode conversion efficiency experimentally measured at 15.5 GHz was

70±20% and at 25 GHz it was 25±10%. A numerical 3-D ray-tracing and full wave EBW mode conversion code<sup>10,11</sup> is used to model B-X-O emission. In Fig. 6 results from the code are compared to measurements at 15.5 GHz for a L-mode discharge. The local EBW emission can be quantified by the radiation temperature  $T_{rad}$  parameter. The measured  $T_{rad}$  agrees with the simulated values within the experimental error for times > 0.2 s. The measured  $C_E$  for 15.5 GHz L-mode emission was 70%, in good agreement with the simulation. However, measurements and simulations are in poor agreement at frequencies of 12 and 25 GHz. Details of the analysis are being investigated to understand the discrepancy. Preliminary analysis of recent EBW emission measurements on H-mode plasmas show  $C_E \approx 0.4$ .

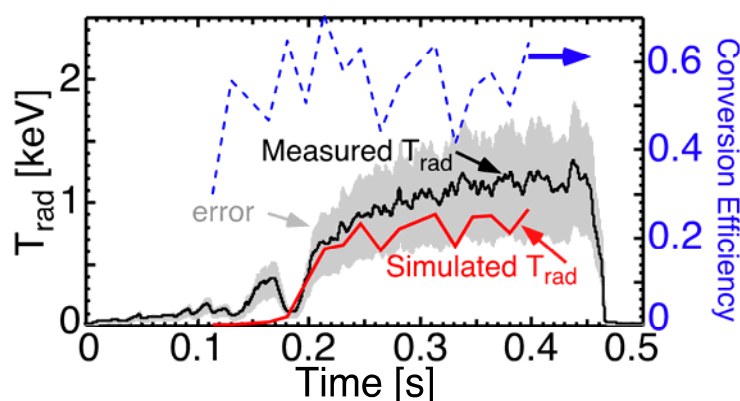


Fig. 6: EBW  $T_{rad}$ : black, measured; red, simulated. Simulated conversion efficiency, dashed blue.

A 28 GHz ECH/EBWH system<sup>12</sup> being installed on NSTX uses a gyrotron with an output power of up to 350 kW for ~ 0.5 s. The ECH will be used to assist non-inductive plasma startup. Feasibility tests are currently being conducted on a low power 28 GHz gyrotron, which normally

operates in TE02 mode, to assess the possibility of operating the gyrotron on in TE01 mode at 15.3 GHz. This frequency would provide fundamental ECH/EBWH near the magnetic axis.

This work is supported by United States DOE contract DE-AC02- 76CH03073.

<sup>1</sup> B.P. LeBlanc et al., Nucl. Fusion 44 (2004) 513–523.

<sup>2</sup> T.M. Biewer et al., Physics of Plasmas 12 (2005) 056108

<sup>3</sup> J.R. Wilson, et al., 16<sup>th</sup> Topical Conf. on RF Power in Plasmas, AIP Conference Proc. 787 (2005) 66.

<sup>4</sup> J.C. Hosea, et al., 16<sup>th</sup> Topical Conf. on RF Power in Plasmas, AIP Conference Proceedings 787 (2005) 82.

<sup>5</sup> J.C. Hosea, et al., 17<sup>th</sup> Topical Conference on RF Power in Plasmas, Clearwater, FL, USA

<sup>6</sup> T.M. Biewer, et al., Rev. Sci. Instrum 75 (2004) 650

<sup>7</sup> J. Preinhaelter and V. Kopecký, J. Plasma Phys. 10, 1 (1973).

<sup>8</sup> S.J. Diem, et al., Rev. Sci. Instrum. 77 (2006)

<sup>9</sup> S.J. Diem et al., Invited talk at 17<sup>th</sup> Topical Conference on RF Power in Plasmas, Clearwater, FL, USA

<sup>10</sup> J. Urban and J. Preinhaelter, Journal of Plasma Physics, 72 (2006)

<sup>11</sup> J. Urban and J. Preinhaelter, Czechoslovak Journal of Physics, 54 (2004)

<sup>12</sup> G. Taylor, et al, 17<sup>th</sup> Topical Conference on RF Power in Plasmas, Clearwater, FL, USA